

Modeling of Laser Supported Detonation Wave Structure Based on Measured Plasma Properties

Keigo Hatai^{*}, Akihiro Fukui[†], Kimiya Komurasaki[‡], and Yoshihiro Arakawa[§]
The University of Tokyo, Kashiwa-shi, Chiba 277-8561, JAPAN

In the Laser Supported Detonation (LSD) regime, pulsed laser energy irradiated to a vehicle is converted to the blast wave enthalpy Based on the measured post-LSD electron number density profiles by the two-wavelength Mach Zehnder interferometer in a line-focusing optics using a 10J/pulse CO₂ laser, electron temperature and absorption coefficient were estimated assuming Local Thermodynamic Equilibrium. As a result, laser absorption was found completed in the layer between the shock front and the electron density peak. Although the LSD-termination timing was not clear from the shock-front/ionization-front separation in the shadowgraph images, there observed drastic changes in the absorption layer thickness from 0.2mm to 0.5mm and in the peak heating rate from 12-17×10¹³W/m³ to 5×10¹³W/m³ at the termination.

NOMENCLATURE

c	=	velocity of light
d	=	thickness of phenomena
e	=	electron charge
h	=	number of fringe shift
k_B	=	Boltzmann constant
K	=	relative refractive index
l	=	thickness of a plasma layer behind a LSD wave
m_e	=	electron mass
n	=	number density
N	=	refractive index
r	=	laser beam spot size
U_i	=	ionization energy
Z	=	partition function
λ	=	wavelength of the light source

Subscripts

n, i, e = neutral particle, ion and electron

I. INTRODUCTION

IN a repetitively pulsed laser propulsion system,^[1-3] a high power laser pulse is beamed toward a vehicle and a shock wave is induced. Thrust is produced by a reflection of the induced shock wave. By a laser beam focused in air, breakdown occurs and a blast wave is generated. Electrons, emanated by the breakdown, absorb the laser energy and are heated. Then the pressure is increased by the collisions between electrons and heavy particles. Through these processes, laser energy is converted into the kinetic energy of the gas. Laser energy is absorbed by the plasma in a laser supported detonation (LSD) regime at the laser intensity higher than 1-10 MW/cm².^[4] In this regime, a

^{*} Graduate student, Department of Aeronautics and Astronautics, The University of Tokyo.
hatai@al.t.u-tokyo.ac.jp

[†] Graduate student, Department of Aeronautics and Astronautics, The University of Tokyo.

[‡] Associate Professor, Department of Advanced Energy, The University of Tokyo, Member AIAA.

[§] Professor, Department of Aeronautics and Astronautics, The University of Tokyo, Member AIAA

ionization front adjoins a shock wave. Because plasma is isometrically heated by a laser beam in a layer close behind the shock wave, the shock wave is driven further. After the plasma region has been separated from a shock wave, plasma is heated isobartically and the shock wave expands almost adiabatically. Therefore, no contribution is expected to the thrust work. Because the LSD regime inevitably terminates with the decay of the laser intensity on the LSD wave, the LSD termination condition is very important for the optimal design of the devices such as the PR laser propulsion.

Typical history of a shock wave and ionization front displacements on the laser axis is shown in Fig.1. The shock wave and the ionization front began to separate, namely the LSD has terminated at about 1.2-1.3 μ s. However, the LSD termination timing is not clear.

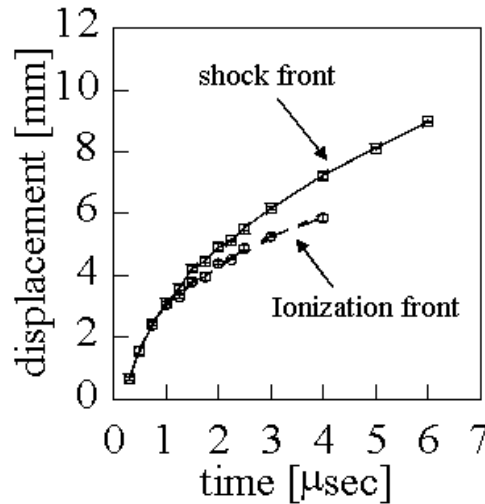


FIGURE 1. Displacements of the shock wave and ionization fronts.

II. MACH-ZEHNDER INTERFEROMETER MEASUREMENT

A TEA CO₂ pulse laser was used. Its nominal energy is 10J/pulse and the beam has the Gaussian distribution on the horizontal axis and trapezoidal distribution on the vertical axis. The laser beam cross-section is a 30mm \times 30mm square.

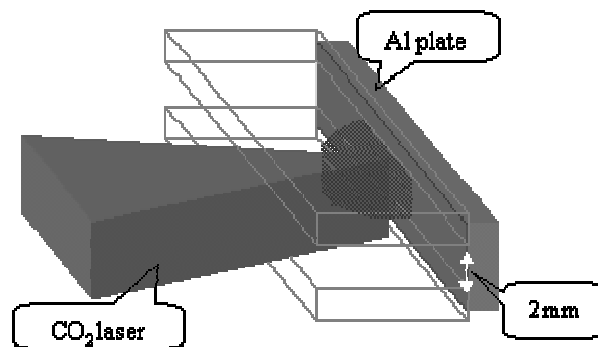


FIGURE 2. Test section for LSD wave visualization.

The laser beam was focused in the horizontal direction using an off-axis line-focusing parabolic mirror whose focal length is 45mm along the optical axis. It reflects an incident laser beam by 90degrees along the optical axis into the focus. The line width on the focal line is estimated at 0.25mm. Because radiation from the plasma seriously disturbed the fringes when the LSD was as thick as 30mm, the laser beam was partially intercepted by a slit to slice

the LSD by 2mm as shown in Fig.2. The top and bottom of the test section were closed with two glass plates to avoid the edge effect. The shock propagation speed and the LSD termination timing were identical in both 30mm-thick and 2mm-thick LSD waves.

The Mach Zehnder interferometer is a non-intrusive and quantitative visualization method, which responds fast enough to acquire non-steady phenomena like a shock wave. The particle number density is measured by counting the shift of fringes. However, the electron density can't be measured by conventional Mach Zehnder interferometer because the shift is a superposition of electron and heavy particle contributions. Using two probe beams, having different wavelengths, the electron number density and heavy particle number density can be separately estimated because only electron-oriented fringes have a wavelength dependency. The measurement optical system is shown in Fig.3. The system denoted by "A" in the figure is different from the conventional Mach Zehnder interferometer. The laser beam was divided into two beams by Beam Splitter #4, and projected on an ICCD camera through band-pass filters (633±1nm and 532±1nm).

Figure 4 shows the Mach Zehnder interferometer images of the LSD. Laser irradiation started to irradiate at $t = 0\mu s$. The displacement of fringes from the baseline is measured on the laser axis: The baseline fringes are interpolated from the side regions which have not been disturbed by the laser heating.

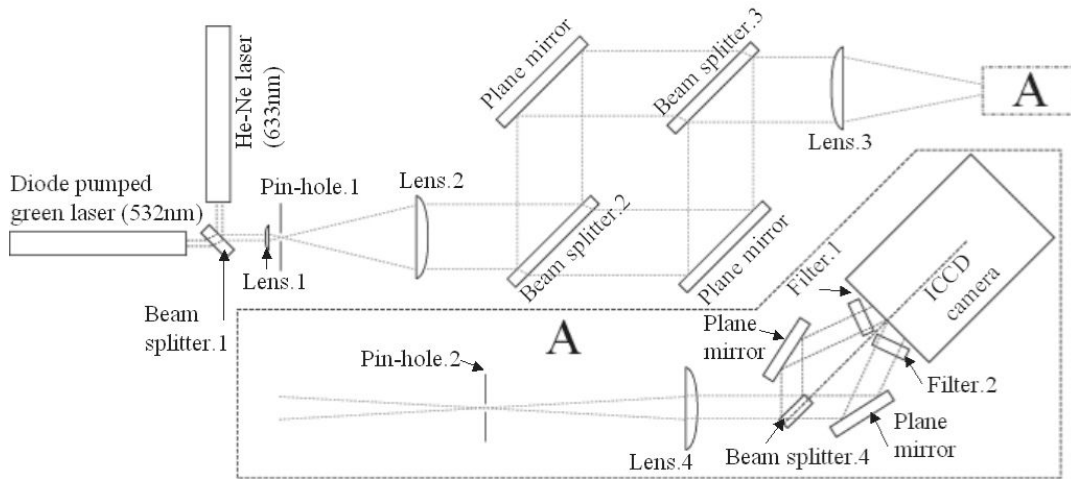


FIGURE 3. Schematic of a two-wavelength Mach-Zehnder interferometer system.

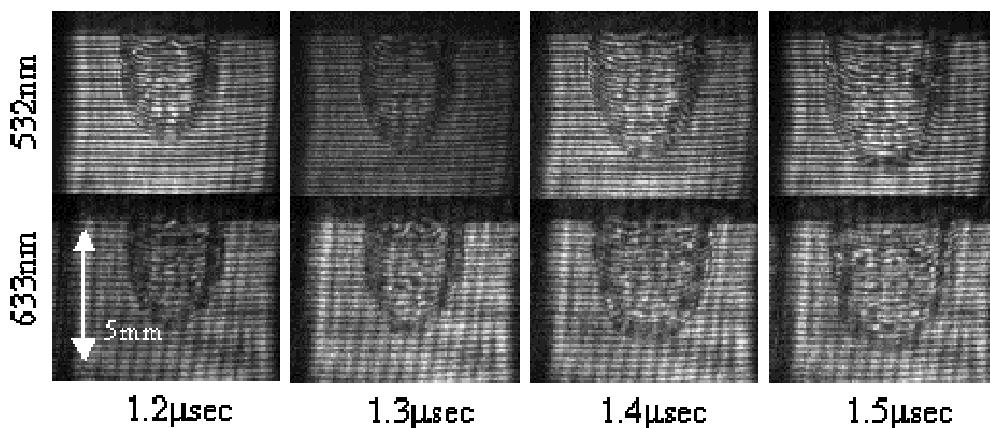


FIGURE 4. Measured interferometer images, top: 532nm, bottom: 633nm.

Figure 5 shows distributions of electron number density and neutral particle density on the laser axis. The LSD has terminated at about 1.3 μs .^[5] The peak density of electron was about $2-2.5 \times 10^{24} m^{-3}$ in the LSD regime and

decreased to about $1.5 \times 10^{24} \text{ m}^{-3}$ after LSD termination. Moreover, the distance between the peak position of electron density and the shock front is gradually increased with time. On the other hand, the neutral particle density profile is almost flat and constant at about $5\text{-}7 \times 10^{25} \text{ m}^{-3}$.

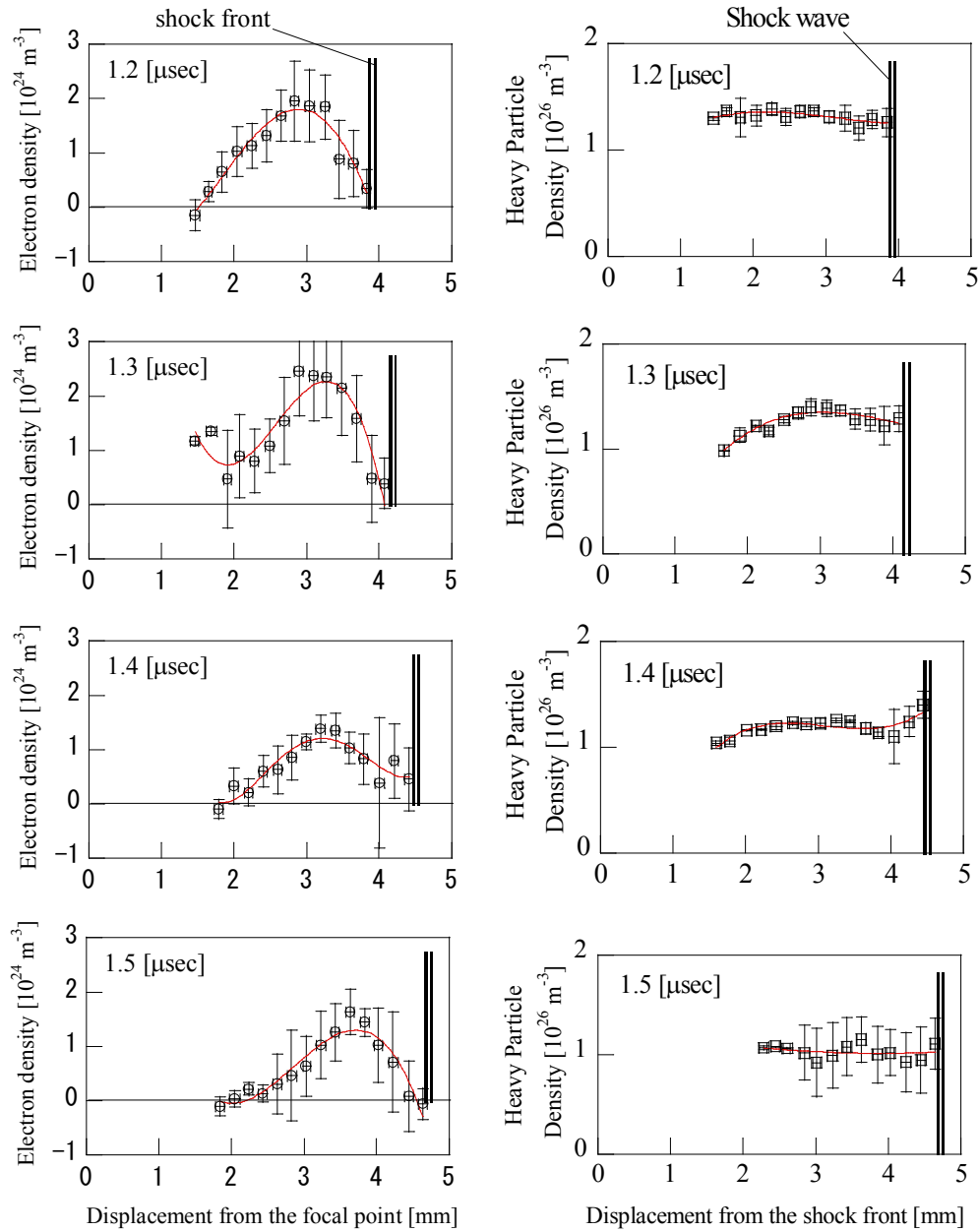


FIGURE 5. Distribution of electron number density (left) and neutral particle density (right). LSD has terminated at about $t \approx 1.3 \mu\text{s}$. A double vertical line indicates the location of a shock front.

III. ENERGY ABSORBING STRUCTURE IN THE LSD WAVE

Assuming Local Thermodynamic Equilibration, electron temperature was estimated using the Saha equation.^{[8],[9]} The electron and neutral particle density profiles were curve-fitted by polynomial functions as shown in Fig.5. The heavy particle temperature is also estimated using the ideal gas equation of state; the pressure profile is assumed flat and same as the spike pressure of a normal shock though the laser heating region. The result is shown in Fig.6.

The electron temperature rose behind the shock front and dropped behind the electron density peak. The maximum electron temperature is about 14000K. The distribution of the electron temperature is not changed so much before and after the LSD termination. The temperature of the heavy particle temperature gradually rose behind the shock front up to 6,000-10,000K, which is still lower than the electron temperature. This indicates that the plasma in the LSD is in strong thermal nonequilibrium between electrons and heavy particles.

The laser energy is absorbed mainly through the inverse Bremsstrahlung effect. The absorption coefficients are expressed as Eqs.(1) and (2).^[10] k_{e-i} and k_{e-n} are respectively related to collisions between electrons and ions and between electrons and neutral particles. These coefficients are calculated using the electron density, neutral particle density and electron temperature. The local laser intensity and absorbed energy are calculated using Eq.(3).

$$k_{e-i} = \sigma_{ei} G n_e n_i \left\{ \exp\left(\frac{h_p c}{\lambda k_B T}\right) - 1 \right\}, \quad \sigma_{ei} = \frac{4}{3} \left(\frac{2\pi}{3m_e k_B T} \right)^{1/2} \frac{e^6 \lambda^3}{h_p c^4 m_e} \quad (1)$$

$$k_{e-n} = \frac{kT^2 A(T) \lambda^3}{h_p c} n_e n_n \left(1 - e^{-h_p c / \lambda k_B T} \right) \quad (2)$$

$$\frac{d(IA_L)}{dx} = (k_{e-n} + k_{e-i}) IA_L, \quad A_L = \frac{d}{f} x \quad (3)$$

Here, G is Gaunt factor, m_e is electron mass, k_B is Boltzmann constant, h_p is Planck constant, c velocity of light, λ is wavelength of CO₂ laser, $A(T)$ is a factor listed in Ref.[8], f and d are the focal length and initial beam width, respectively.

The laser heating rate and local laser intensity are estimated and plotted in Fig.7. Local laser power IA_L is normalized by incident laser power and electron density is normalized by the peak electron density. It is found that the laser absorption has been completed by the electron density peak.

Figure 8 shows the histories of laser heating rate. The peak of laser heating rate is $12-17 \times 10^{13} \text{W/m}^3$ in LSD regime and the heating rate decreases to $5 \times 10^{13} \text{W/m}^3$ thorough the LSD termination. The absorption layer thickness, defined as the distance from the shock front to the position which local laser power decreases by $1/e$, is also plotted in Fig.8. At the LSD termination, the absorption layer got thicker drastically. The changes in parameters before and after LSD termination are tabulated in Table 1.

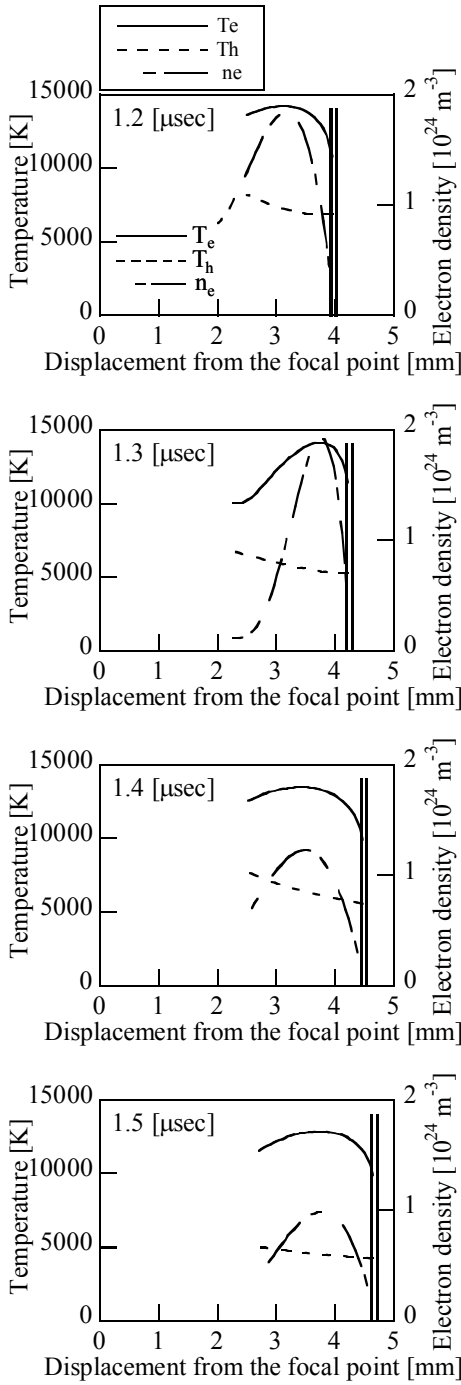


FIGURE 6. Electron and heavy particle temperatures. LSD terminated at about $1.3\mu\text{s}$. A double vertical line shows the location of a shock front.

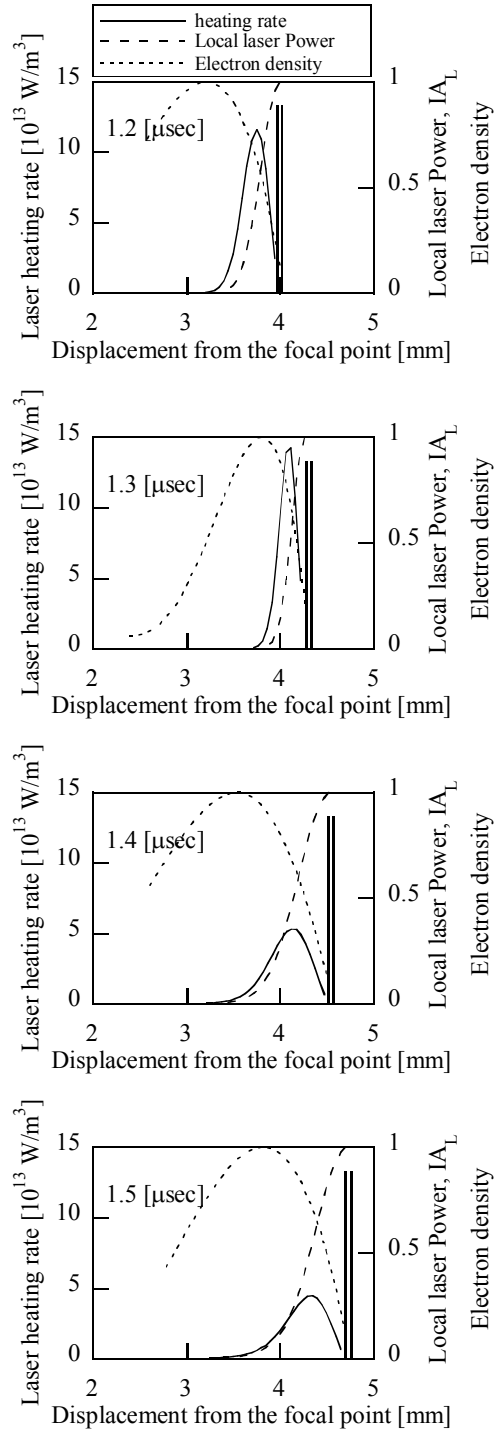


FIGURE 7. Laser heating rate and local laser power. A double vertical line shows the location of a shock front.

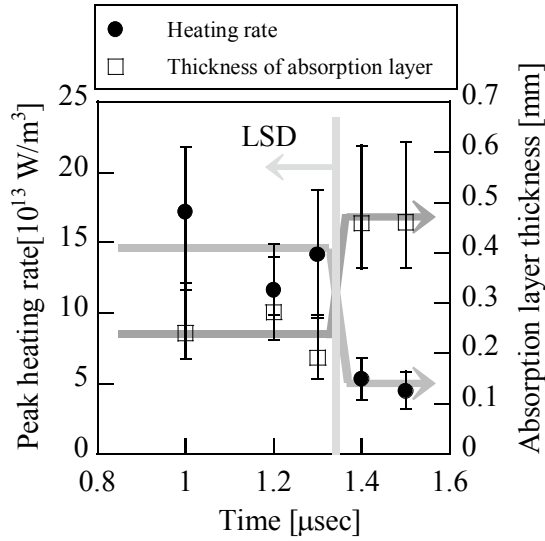


FIGURE 8. Histories of laser heating rate and the absorption layer thickness.

TABLE 1. Comparison of the properties in the LSD layer before and after the LSD termination.

properties	before	after
local laser intensity, MW/cm 2		3
Mach number		6.5
peak electron number density, m $^{-3}$	2-2.5 $\times 10^{24}$	1.5 $\times 10^{24}$
peak heating rate, W/m 3	12-17 $\times 10^{13}$	5 $\times 10^{13}$

IV. CONCLUSION

- Through the LSD termination, the electron peak density was decreased from 2-2.5 $\times 10^{24}$ m $^{-3}$ to 1.5 $\times 10^{24}$ m $^{-3}$. On the other hand, the neutral particle density profile is almost flat and constant at about 5-7 $\times 10^{25}$ m $^{-3}$.
- The laser energy was found fully absorbed by the electron density peak.
- The peak of laser heating rate decreased drastically through the LSD termination from 12-17 $\times 10^{13}$ W/m 3 to 5 $\times 10^{13}$ W/m 3 .
- Absorption layer thickness also got longer drastically after the LSD termination from 0.2-0.3mm to 0.5mm.

REFERENCES

1. Kantrowiz. A., Propulsion to Orbit by Ground Based Lasers, Aeronaut. Astronaut., 10(1972), pp.74-76
2. Myrabo, L.M., Messit, D.G., and Mead, F. B. Jr., AIAA paper 98-1001, 1998
3. Katsurayama, H., Komurasaki, K., and Arakawa, Y., J. Space Tech. Sci. 20(2): 32-42, 2005
4. Mori, K., Komurasaki, K., and Arakawa, Y., J. Spacecraft and Rockets 41(5): 887-889, 2004
5. Mori, K., Komurasaki, K. and Arakawa, Y.: Influence of the Focusing f Number on the Heating Regime Transition in Laser Absorption Waves, J. of Appl. Phys., 15, (2002), pp.5663-5667.
6. Mori, K., Komurasaki, K. and Arakawa, Y.: Energy Transfer from a Laser Pulse to a Blast Wave in Reduced-Pressure Air Atmospheres, J. of Appl. Phys., 95, (2004), pp.5979-5983.
7. Ushio, M., Katsurayama, H., Kawamura, K., Komurasaki, K., Koizumi, K., and Arakawa, Y., Energy conversion process in Laser Supported Detonation waves driven by a linearly focused laser beam, IAC paper 05-C4.6.04, 2005

8. F. F. Chen., Introduction to Plasma Physics and Controlled Fusion, Plenum Publishers, 1984, pp. 1
9. Y. B. Zeldovich, Y. P. Raizer, Physics of Shock Waves and High-Temperature Hydrodynamic Phenomena, Dover Publications, 1966, pp. 192-197, 444
10. N. H. Kemp., and P. F. Lewis., Laser-heated Thruster, NASA CR-161665, 1980